Available online at www.sciencedirect.com
SCIENCE DIRECT®
Journal of the European Ceramic Society 24 (2004) 3617–3622
www.elsevier.com/locate/jeurceramsoc

Compositional and processing effects on electrical properties of $(Ba_{0.85}Pb_{0.15})TiO_3$-based positive temperature coefficient resistors

Zeming He [a,*], J. Ma [a], Yuanfang Qu [b], Chenggang Wang [b]

[a] *School of Materials Engineering, Nanyang Technological University, Nanyang Avenue, Singapore 639798, Singapore*
[b] *Materials Institute, Tianjin University, Tianjin 300072, PR China*

Received 22 July 2003; received in revised form 1 December 2003; accepted 7 December 2003

Available online 13 April 2004

Abstract

In the present work, $(Ba_{0.85}Pb_{0.15})TiO_3$-based positive temperature coefficient resistors (PTCRs) with low room-temperature resistivities were produced, and the effects of composition and processing conditions on materials electrical properties were investigated. For (Ba,Pb)TiO_3-based ceramics, it was noted that an addition of double donors $Sb_2O_3 + Nb_2O_5$ led to a lower room-temperature resistivity than that of single donor Nb_2O_5. The resistivity followed to reduce when properly increasing the donor concentration and decreasing the acceptor (MnO_2) concentration. The correlation of sintering temperature with ceramic parameters, namely, density, grain size, room-temperature resistivity, resistivity jump, and room-temperature breakdown strength, was discussed. Metal Cr was added to ceramic matrix to further reduce the resistivity. A reducing sintering and a subsequent oxidation treatment processes were employed, and the influences of metallic content and processing conditions on composite density, room-temperature resistivity, and room-temperature breakdown strength were analyzed. Low room-temperature resistivity PTCRs were produced by controlling both Cr content and the processes.

Keywords: (Ba,Pb)TiO_3; PTCR; Electrical resistivity; Resistors

1. Introduction

In ferroelectric materials, positive temperature coefficient (PTC) effect is a phenomenon related to ferroelectric phase transformation, grain-boundary barrier, and semiconducting grain.[1] Compared with the lower resistance in ferroelectric state at room temperature, several orders of magnitude of resistance jump is exhibited when the material is heated through its Curie point.[2] Positive temperature coefficient resistors (PTCRs) have been extensively used as over-current limiters, self-regulating heaters, and temperature sensors.[3] The over-current limiter has attracted more attention because it can provide the protection, and hence the improvement on safety and reliability of the products. However, a challenge is faced for this application, especially in microelectronic circuits work at low voltage, due to the relatively high room-temperature resistivity.[4] Therefore, an effort to reduce the room-temperature resistivity of PTC materials is indispensable.

Barium titanate and its related compounds are ideal candidates for producing various PTC components due to their high temperature coefficient of resistance.[5] The addition of the trivalent (La^{3+}, Sb^{3+}, Y^{3+})[5–11] or pentavalent (Nb^{5+}, Ta^{5+})[12–14] donor dopants increases the room-temperature conductivity.[15] On the other hand, as acceptor dopants, Mn^{2+} or Mn^{4+} ions[5,10] are also usually added in PTC materials. The acceptors are expected to locate at the grain boundaries to enhance PTC effect.[16,17]

For the ultimate goal of fabricating low room-temperature resistivity PTC device to meet the requirement of over-current limiter at low voltage, in the present work, the studies of compositional and processing effects on electrical properties of the $(Ba_{0.85}Pb_{0.15})TiO_3$-based materials are reported. $Sb_2O_3 + Nb_2O_5$ double donors were added, and the concentrations of donor and acceptor were also adjusted. The correlation of composition and sintering temperature with materials density, grain size, room-temperature resistivity, resistivity jump, and room-temperature breakdown strength is discussed. To further reduce the room-temperature resistivity, metal Cr was added to a selected low resistivity ceramic matrix. A sintering in a reducing atmosphere and a

* Corresponding author. Tel.: +65-67904590; fax: +65-67909081.
E-mail address: zmhe@ntu.edu.sg (Z. He).

0955-2219/$ – see front matter © 2004 Elsevier Ltd. All rights reserved.
doi:10.1016/j.jeurceramsoc.2003.12.015

subsequent oxidation treatment processes were used to form composites. The influence of Cr content and processing conditions on composite density, room-temperature resistivity, and room-temperature breakdown strength is presented.

2. Experimental procedure

2.1. Raw materials

Commercially available reagent-grade powders were used as the starting materials. $BaCO_3$, Pb_3O_4, and TiO_2 were used to form (Ba,Pb)TiO_3. Sb_2O_3, Nb_2O_5, MnO_2, BN, Al_2O_3, SiO_2, TiO_2, and Cr were added for property modification.

2.2. Processing

Table 1 shows the designed materials compositions, where AST indicates a mixture of Al_2O_3, SiO_2, and TiO_2. Throughout the present work, the materials prepared are termed as Samples 1–8 based on the compositions shown in the table. The powders and dopants for each composition were mixed for 24 h in a Restch planetary ball mill. The resultant slurry was dried in an oven and then the powders were calcined at 1000 °C for 2 h in a Carbolite high temperature furnace. Other additives were mixed with the powders which were ball milled and dried again. The dried powders were pressed at 180 MPa to form pellets. The compacts (Samples 1–3) were sintered in air at different temperatures (1170–1200 °C) for 20 min. The Cr-containing compacts (Samples 4–8) were first sintered at 1180 °C for 20 min in a carbon reducing atmosphere, which was created by covering the compacts with graphite powders. They were then oxidized in air at 600 °C for 20 min. The heating and cooling rates for all the samples were 10 and 15 °C/min, respectively.

2.3. Characterization

The densities of the samples were measured using Archimedes method. A Regaku X-ray diffractometer and a JEOL scanning electron microscope were used to reveal the phases and the microstructures of the samples. The average grain size of the sample was estimated from the SEM image. For the characterization of the electrical properties, both ends of the sample were applied with the silver pastes to form the Ohmic contact. A KATO X-Y multifunctional electrical testing apparatus was used to measure room-temperature (25 °C) resistivity, room-temperature breakdown strength, and resistivity–temperature curve.

Table 1
Designed materials compositions: $(Ba_{0.85}Pb_{0.15})TiO_3$ + 0.04BN + 0.1 wt.% AST with different contents of dopants and metal

Number	Additive			
	Sb_2O_3 (mol)	Nb_2O_5 (mol)	MnO_2 (mol)	Cr (wt.%)
1	0	0.0013	0.0004	0
2	0.0002	0.0011	0.0004	0
3	0.0004	0.0011	0.0003	0
4	0.0004	0.0011	0.0003	5
5	0.0004	0.0011	0.0003	10
6	0.0004	0.0011	0.0003	15
7	0.0004	0.0011	0.0003	20
8	0.0004	0.0011	0.0003	25

3. Results and discussion

3.1. Dopant

Fig. 1 shows the variations of room-temperature resistivity as a function of sintering temperature for Samples 1–3. In the investigated sintering temperature range, it can be seen that, at a fixed sintering temperature, the room-temperature resistivity of Sample 1 is the highest, next that of Sample 2, and that of Sample 3 is the lowest. The resistivity difference in samples at a given sintering temperature is mainly attributed to the doping effect. In general, either Sb_2O_3 or Nb_2O_5 added could lead to semiconducting grains. When the two dopants were added simultaneously, Ba^{2+} and Ti^{4+} were substituted by Sb^{3+} and Nb^{5+}, respectively, based on their ionic radii. The defect reactions are:

$$x\mathrm{Sb_2O_3} + 2\mathrm{BaTiO_3} = 2(\mathrm{Ba_{1-x}}^{2+}\mathrm{Sb}_x^{3+})[\mathrm{Ti_{1-x}}^{4+}(\mathrm{Ti}^{4+}\cdot \mathrm{e})_x]\mathrm{O_3} + \frac{x}{2}\mathrm{O_2} + 2x\mathrm{BaO} \quad (1)$$

and

$$y\mathrm{Nb_2O_5} + 2\mathrm{BaTiO_3} = 2\mathrm{Ba}^{2+}[\mathrm{Ti_{1-2y}}^{4+}\mathrm{Nb}_y^{5+}(\mathrm{Ti}^{4+}\cdot \mathrm{e})_y]\mathrm{O_3} + \frac{y}{2}\mathrm{O_2} + 2y\mathrm{TiO_2} \quad (2)$$

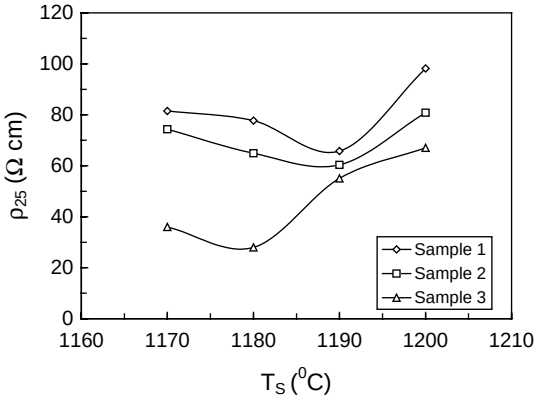

Fig. 1. Variations of room-temperature resistivity (ρ_{25}) with sintering temperature (T_S) of Samples 1–3.

Therefore, for $Sb_2O_3 + Nb_2O_5$ doping material system, both reactions contributed to the semiconducting process simultaneously, which led to a higher entropy of the lattice system and hence a higher reaction activity of grains. In addition, donor energy levels were created at both Ba and Ti sites, which resulted in a higher effective donor concentration compared with the single donor doping, though the added donor concentrations were same for the two compositions. Furthermore, based on Eqs. (1) and (2), the resultant BaO and TiO_2 could react to form $BaTiO_3$ and continue to be involved in the semiconducting reactions, which made a complete and thorough substitutive reaction. A lower room-temperature resistivity is achieved by double donors doping due to a better grain semiconducting process occurred. In both of Samples 2 and 3, double donors $Sb_2O_3 + Nb_2O_5$ were added. However, compared with Sample 2, more donor and less acceptor were doped in Sample 3, which led to a lower room-temperature resistivity. It is noted that the adjustment of the amounts of donor and acceptor should be appropriate, because the resistivity would increase if large amount of donors are added.[18] With respect to Fig. 1, the room-temperature resistivity values of Samples 1–3 in the investigated sintering temperature range are less than 100.00 Ω cm, and the one of Sample 3 sintered at 1180 °C is 28.00 Ω cm. The achieved values are relatively low for $BaTiO_3$-based PTC ceramics, as reported in the literature.[4,19]

The resistivity-temperature curves of Samples 1–3 sintered at 1180 °C are shown in Fig. 2. It can be seen that all the samples exhibit PTC effect. Samples 1 and 3, respectively, have the largest and the smallest resistivity jumps. For PTC materials, the resistivity jump near the Curie temperature is related to the grain-boundary barrier, and higher grain-boundary barrier leads to larger resistivity jump.[16] The value of the grain-boundary barrier is in direct proportion to the acceptor state density and in inverse proportion to the square of the effective donor concentration.[20] For Sample 1, higher acceptor and lower donor concentrations resulted in higher resistivity jump, while for Sample 3, lower acceptor and higher donor concentrations resulted in lower resistivity jump. With respect to Fig. 2, the Curie temperature for all the samples was determined as 180 °C. The higher Curie temperature, compared with 120 °C of pure $BaTiO_3$, is attributed to the addition of Pb ions to form $(Ba,Pb)TiO_3$ solid solution.[21]

3.2. Sintering temperature

From compositional design, Sample 3 has achieved low room-temperature resistivity. In addition to composition, sintering is the key process to determine PTC materials properties, and the selection of sintering temperature, sintering atmosphere, and cooling rate is important. It is well known that the PTC effect could exhibit when sintering in air, but it could diminish when sintering in a reducing ambient.[20] The processes of a reducing or neutral atmosphere sintering, followed by an oxidation treatment were also reported to fabricate PTC ceramics[11,22,23]. Fast cooling rate is required for achieving low room-temperature resistivity.[24] In the present work, the sintering process was actually designed from these basic concepts to achieve low room-temperature resistivity PTC materials.

The SEM image of Sample 3 sintered at 1180 °C is shown in Fig. 3, which is an illustration to show the microstructure of the sintered PTC ceramic, and, as mentioned, the grain size can be estimated from it. Fig. 4 shows the variations of density and grain size with sintering temperature of Sample 3. It can be seen that the most suitable sintering temperature is 1180 °C at which highest density and moderate grain size is obtained.[11] 1190 °C is also appropriate just a slight decrease of the density. At 1170 °C, the sample could be somewhat under-sintered due to low density and small grain size. At 1200 °C, on the contrary, the sample could be somewhat over-sintered due to low density caused by lead volatilization and large grain size related to abnormal growth.

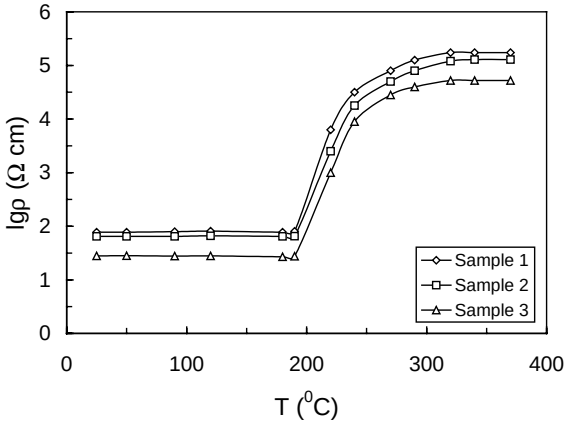

Fig. 2. Resistivity ($lg\rho$)–temperature (T) curves of Samples 1–3 sintered at 1180 °C.

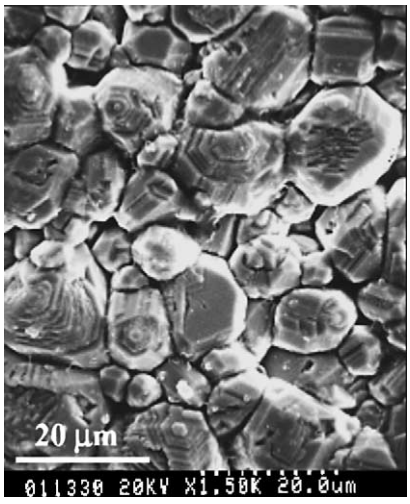

Fig. 3. SEM image of Sample 3 sintered at 1180 °C.

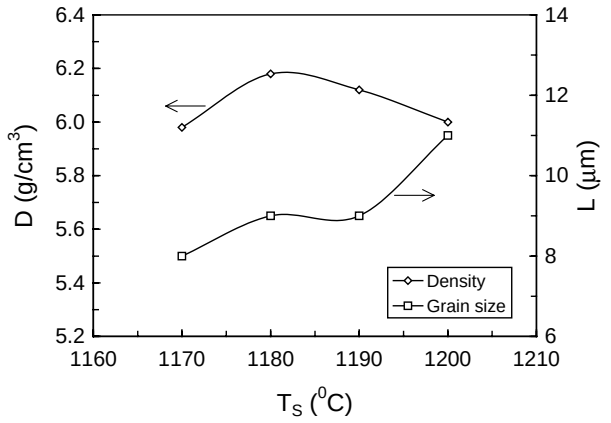

Fig. 4. Variations of density (D) and grain size (L) with sintering temperature (T_S) of Sample 3.

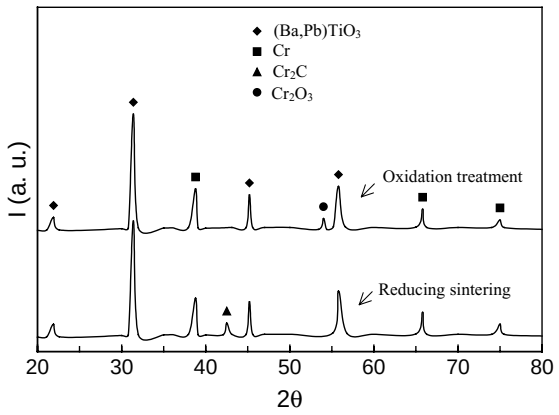

Fig. 6. XRD traces of Sample 5 after reducing sintering and oxidation treatment.

Fig. 5 shows the variations of the resistivity jump and the room-temperature breakdown strength with sintering temperature of Sample 3. The resistivity jump and the room-temperature breakdown strength all increase with the sintering temperature up to maxima at 1190 °C and then decrease. With respect to Fig. 1, 1180 °C is the temperature for achieving resistivity minimum. It is noted that the components sintered at these two temperatures possess high density and moderate grain size, as shown in Fig. 4. Low room-temperature resistivity and high resistivity jump, however, are difficult to obtain at one fixed sintering temperature for a PTC ceramic. This phenomenon is consistent with that reported by Zhao et al.[25] when they sintered (Sr,Pb)TiO_3-based ceramics. The mechanisms for reducing room-temperature resistivity and for enhancing PTC effect are antagonistic, and improving one parameter leads to sacrificing another one. The effect of sintering temperature on the room-temperature breakdown strength of Sample 3 is actually the combining results of materials density, grain size, and resistivity. The maximum of strength at 1190 °C is attributed to higher density, moderate grain size, and higher room-temperature resistivity.

In general, the temperature reported for sintering PTC ceramics was above 1300 °C.[7,10] In the present work, the sintering temperature range is 1170–1200 °C. Therefore, PTC materials were obtained at lower sintering temperatures, which is mainly attributed to the addition of BN.[4,19,26]

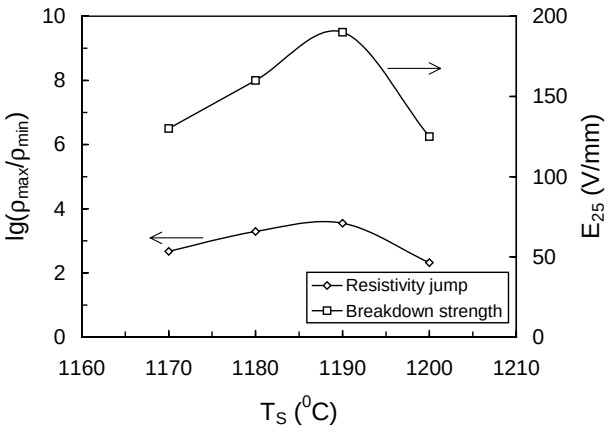

Fig. 5. Variations of resistivity jump ($lg(\rho_{max}/\rho_{min})$) and room-temperature breakdown strength (E_{25}) with sintering temperature (T_S) of Sample 3.

3.3. Cr addition

As discussed in Section 3.1, Sample 3 sintered at 1180 °C achieved relatively low room-temperature resistivity. To further reduce the resistivity, metal Cr was added in the ceramic matrix of Sample 3. A reducing sintering at 1180 °C and a subsequent oxidation at 600 °C (to enhance PTC effect) were used to form composites (Samples 4–8). As an illustration, the XRD traces of Sample 5 are shown in Fig. 6. In addition to the detected (Ba,Pb)TiO_3 and Cr, a peak of Cr_2C was found after reducing sintering. The formation of Cr_2C is attributed to the reaction between Cr and graphite when the compact was covered with graphite powders during reduction sintering. After oxidation treatment, a Cr_2O_3 peak was identified due to the oxidation of some amount of metal Cr.

Fig. 7 shows the variations of density with Cr content after reducing sintering and oxidation treatment. Among the composites, Sample 6 achieves the highest density after reducing sintering, which indicates a good densification behavior of this sample when compared with others. After oxidation treatment, the density decreases with the increase of Cr content. If the density values after reducing sintering and oxidation treatment of the same sample are compared, it is shown that the density after oxidation is less than the one before oxidation, except that of Sample 4. From reduction sintering to oxidation treatment, the density change of the composite is related to two processes. One is the density-increasing tendency, which is caused by the weight increase resulting from the absorbed oxygen when forming Cr_2O_3 on some amount of Cr surfaces, as detected in Fig. 6. Another is the density-decreasing tendency, that is, a compressive stress is

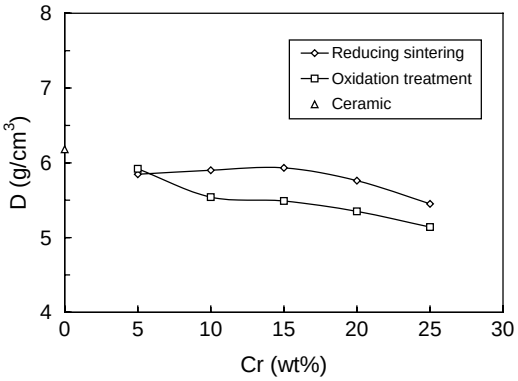

Fig. 7. Variations of density (D) with Cr content after reducing sintering and oxidation treatment.

acted on ceramics, which is caused by the volume expansion of Cr during oxidation. Near the stress zone, crack and pores could be formed, which leads to a loose structure, thus lowering materials density. The density change, therefore, is the result of the interaction between the abovementioned two processes. In our earlier work,[27] the microstructures of the sample before and after oxidation were shown. As a result, for Sample 4, the first process would take main effect, so that its density turns higher after oxidation. For the other samples, the second process would dominate gradually as Cr content increases, and therefore lower density occurs after oxidation treatment. In Fig. 7, the density of Sample 3 (zero Cr content) sintered at 1180 °C is also shown for comparison. It should be noted that the composite density, whether before oxidation or after oxidation, is less than that of the ceramic. This is mainly attributed to the densification retardation occurred during sintering of composite when Cr was introduced.[28]

The variations of room-temperature resistivity with Cr content of the composites are shown in Fig. 8. The resistivity measured after reducing sintering decreases with increasing Cr content. In general, the resistivity of the composite is the total sum of ceramic resistivity, metal resistivity, and the resistivity of interface between ceramic and metal. In our previous work,[27] an Ohmic contact between ceramic (Ba,Pb)TiO_3 and metal Cr was reported. As metallic content increases, the resistance contribution of metal to composite increases and leads to the decreased resistivity. One issue should be pointed out that the resistivities of Samples 4 and 5 after reduction sintering are very high, even higher than that of Sample 3 (its value also in Fig. 8). This could be attributed to the Cr ions in Cr_2C, as identified in Fig. 6. The Cr ions diffused into ceramic grains and compensated some donors, and as a result the grain semiconducting behavior was weakened remarkably. After oxidation treatment, the trend of resistivity changing with Cr content is same as that of reducing sintering. However, the value is higher than that of reducing sintering for a fixed composite. This is attributed to some amount oxidation of Cr, for the resistivity of Cr is lower than that of Cr_2O_3. From Fig. 8, the room-temperature resistivities of Samples 6–8 prepared from the entire processes are 1.76–16.70 Ω cm. Therefore, in the present work, more relatively low resistivities have been achieved by adjusting Cr content from 15 to 25 wt.% and the processes of reducing sintering and oxidation treatment.[4,19] In addition, it was reported in our earlier work[27] that PTC effect was also shown for Samples 6–8 after oxidation treatment, compared with negative temperature coefficient (NTC) effect of Samples 4 and 5.

Fig. 9 shows the variations of room-temperature breakdown strength with Cr content of the composites. For comparison, the breakdown strength of ceramic Sample 3 is also included. In composites, a nearly flat variation of the reducing sintered breakdown strength with Cr content covering Samples 4–6 is seen, and then it decreases with the increase of Cr content. It is noted that the composite room-temperature breakdown strength investigated is related to the density and the room-temperature resistivity. High density and high resistivity could lead to high breakdown strength. With respect to Figs. 7 and 8, the occurrence of the flat line is attributed to the compromise of the changes of both density and resistivity with Cr content, because density increases and resistivity decreases

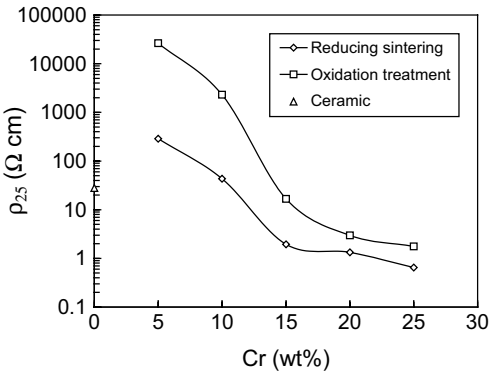

Fig. 8. Variations of room-temperature resistivity (ρ_{25}) with Cr content after reducing sintering and oxidation treatment.

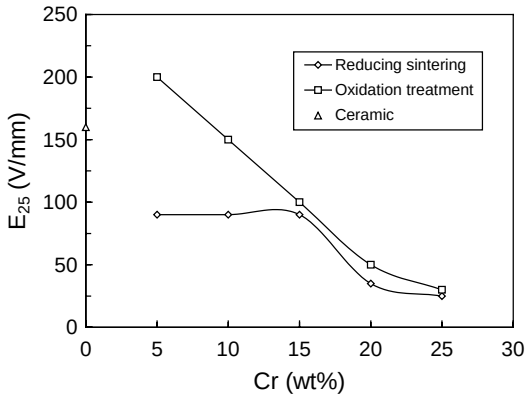

Fig. 9. Variations of room-temperature breakdown strength (E_{25}) with Cr content after reducing sintering and oxidation treatment.

with the increase of Cr. As metallic content continues to increase (from Samples 7 to 8), both density and resistivity decrease, as a result, breakdown strength also decreases. After oxidation treatment, the breakdown strength of the composite decreases with the increase of Cr content. This is explained that both lower and lower density and resistivity are obtained as Cr content increases. For all the investigated samples, the room-temperature breakdown strength of Sample 4 after oxidation is the highest, and this is resulted from its highest resistivity and highest density in the composites. The breakdown strength of ceramic Sample 3 ranks next to that of Sample 4, which is mainly attributed to its highest density in all the samples.

4. Conclusions

This paper reports the effects of composition and processing on the electrical properties of $(Ba_{0.85}Pb_{0.15})TiO_3$-based PTCR. The materials parameters investigated include density, grain size, resistivity jump, room-temperature breakdown strength, and room-temperature resistivity.

Compared with single donor Nb_2O_5, lower room-temperature resistivity is achieved by the addition of double donors $Sb_2O_3 + Nb_2O_5$. The resistivity continues to reduce when trace concentrations of donor and acceptor are, respectively, increased and decreased.

The $Sb_2O_3 + Nb_2O_5$ doped (Ba,Pb)TiO_3 PTC ceramic sintered at 1180 °C achieves the lowest room-temperature resistivity of 28.00 Ω cm.

For (Ba,Pb)TiO_3–Cr composites, the material with both low room-temperature resistivity and PTC effect was obtained by adjusting the added Cr content and the processes of reducing sintering at 1180 °C and oxidation treatment at 600 °C. The PTC composite with 25 wt.% Cr has the lowest room-temperature resistivity of 1.76 Ω cm.

References

1. Haertling, G. H., Ferroelectric ceramics: history and technology. *J. Am. Ceram. Soc.* 1999, **82**, 797–818.
2. Newnham, R. E. and Ruschau, G. R., Smart electroceramics. *J. Am. Ceram. Soc.* 1991, **74**, 463–480.
3. Uchino, K., *Ferroelectric Devices*. Marcel Dekker Inc., New York, 2000.
4. Huang, Z. Z., Adikary, S. U., Chan, H. L. W. and Choy, C. L., Preparation and properties of PTCR ceramics with low resistivity sintered at low temperature. *J. Mater. Sci. Mater. Electron.* 2002, **13**, 221–224.
5. Chatterjee, S., Sengupta, K. and Maiti, H. S., A miniature PTC thermistor based sensor element fabricated by tape casting technique. *Sens. Actuators B* 1999, **60**, 155–160.
6. Kleint, C. A., Stoepel, U. and Rost, A., X-ray diffraction and conductivity investigations of lanthanum-doped barium titanate ceramics. *Phys. Status Solidi A* 1989, **115**, 165–172.
7. Voltzke, D., Abicht, H.-P., Pippel, E. and Woltersdorf, J., Ca-containing additives in PTC-$BaTiO_3$ ceramics: effects on the microstructural evolution. *J. Eur. Ceram. Soc.* 2000, **20**, 1663–1669.
8. Chen, L.-F. and Tseng, T.-Y., Grain-boundary surface states of (Ba,Pb)TiO_3 positive temperature coefficient ceramics doped with different additives and its influence on electrical properties. *IEEE. T. Compon. Pack. Manu. A* 1996, **19**, 423–430.
9. Ho, I.-C. and Hsieh, H.-L., Low temperature fired positive temperature coefficient resistors. *J. Electron. Mater.* 1994, **23**, 471–476.
10. Ozawa, M. and Suzuki, S., Influence of heat treatment with nitrogen in positive-temperature-coefficient-type $BaTiO_3$. *J. Mater. Sci. Lett.* 1997, **16**, 545–546.
11. Osonoi, A., Tashiro, S. and Igarashi, H., Effect of A-site substitution and firing temperature on microstructure and electrical properties of $BaTiO_3$ semiconducting ceramics fired by reduction–reoxidation method. *Jpn. J. Appl. Phys.* 1997, **36**, 6021–6026.
12. Zajc, I. and Drofenik, M., Semiconducting $BaTiO_3$ ceramic prepared by low temperature liquid phase sintering. *J. Mater. Res.* 1998, **13**, 660–664.
13. Gillot, C., Michenaud, J.-P., Baukens, I. and Duvigneaud, P.-H., Microscopic original of the PTC effect in niobium-doped barium titanate. *J. Am. Ceram. Soc.* 1997, **80**, 1043–1046.
14. Fu, S.-L., Ho, I.-C. and Chen, L.-S., Studies on semiconductive $(Ba_{0.8}Sr_{0.2})(Ti_{0.9}Zr_{0.1})O_3$ ceramics. *J. Mater. Sci.* 1990, **25**, 4042–4046.
15. Morrison, F. D., Coats, A. M., Sinclair, D. C. and West, A. R., Charge compensation mechanisms in La-doped $BaTiO_3$. *J. Electroceram.* 2001, **6**, 219–232.
16. Heywang, W., Barium titanate as semiconductor with blocking layers. *Solid State Electron.* 1961, **3**, 51–58.
17. Jonker, G. H., Some aspects of semiconducting barium titanate. *Solid State Electron.* 1964, **7**, 895–903.
18. Al-Shahrani, A. and Abboudy, S., Positive temperature coefficient in Ho-doped $BaTiO_3$ ceramics. *J. Phys. Chem. Solids* 2000, **61**, 955–959.
19. Huang, Z. Z., Adikary, S. U. and Chan, H. L. W., Processing characteristics of PTCR ceramics with low sintering temperature. *J. Mater. Sci. Mater. Electron.* 2002, **13**, 605–608.
20. Ho, I.-C. and Fu, S.-L., Effect of reoxidation on the grain-boundary acceptor-state density of reduced $BaTiO_3$ ceramics. *J. Am. Ceram. Soc.* 1992, **75**, 728–730.
21. Feng, J., Relation between Curie-temperature of $BaTiO_3$ PTC ceramic and its additives. *J. Funct. Mater.* 1996, **27**, 421–423.
22. Kanda, A., Tashiro, S. and Igarashi, H., Effect of firing atmosphere on electrical properties of multilayer semicondcucting ceramics having positive temperature coefficient of resistivity and Ni–Pd internal electrodes. *Jpn. J. Appl. Phys.* 1994, **33**, 5431–5434.
23. Urek, S. and Drofenik, M., PTCR behavior of highly donor doped $BaTiO_3$. *J. Eur. Ceram. Soc.* 1999, **19**, 913–916.
24. Yoon, S. H. and Kim, H., Space charge segregation during the cooling process and its effect on the grain boundary impedance in Nb-doped $BaTiO_3$. *J. Eur. Ceram. Soc.* 2002, **22**, 689–696.
25. Zhao, J., Li, L. and Gui, Z., Influence of microstructure on the properties of $Sr_{0.5}Pb_{0.5}TiO_3$ V-shaped PTCR. *Ceram. Int.* 2002, **28**, 261–264.
26. He, Z., Ma, J., Qu, Y. and Xue, F., Effect of additives on the electrical properties of a $(Ba_{0.92}Sr_{0.08})TiO_3$-based positive temperature coefficient resistor. *J. Eur. Ceram. Soc.* 2002, **22**, 2143–2148.
27. He, Z., Ma, J., Qu, Y. and Wang, C., A structural model of Cr/(Ba,Pb)TiO_3 positive temperature coefficient composite. *J. Mater. Sci. Mater. Electron.* 2000, **11**, 235–238.
28. Maekawa, K., Nakada, Y. and Kimura, T., Origins of hindrance in densification of Ag/Al_2O_3 composites. *J. Mater. Sci.* 2002, **37**, 397–410.